

M. Arnould[†])

Institut d'Astronomie et d'Astrophysique, Université Libre de Bruxelles, Belgium

F. Tondeur

Institut Supérieur Industriel de Bruxelles, and Université Libre de Bruxelles, Belgium

Abstract

Nuclear level density calculations are performed using a model of fermions interacting via the pairing force, and a realistic single particle potential. The pairing interaction is treated within the BCS approximation with different pairing strength values. The single particle potentials are derived in the framework of an energy-density formalism which describes self-consistently the ground states of spherical nuclei. These calculations are extended to statically deformed nuclei, whose estimated level densities include rotational band contributions. The theoretical results are compared with various experimental data. In addition, the level densities for several nuclei far from stability are compared with the predictions of a back-shifted Fermi gas model. Such a comparison emphasizes the possible danger of extrapolating to unknown nuclei classical level density formulae whose parameter values are tailored for known nuclei.

1. Introduction

The nuclear level density is a quantity of fundamental importance in many calculations and analyses of experimental data. A lot of studies have been devoted to its evaluation since Bethe's pioneering work¹⁾ (see e.g. refs.²⁻⁴⁾ for reviews).

By far, the so-called partition function method is the most widely used technique for calculating level densities, particularly in view of its ability to provide closed analytical formulae at the expense of some approximations. The prototype of those expressions is the famous Bethe formula for the level density of a gas of noninteracting fermions confined to the nuclear volume, and having equally spaced energy levels¹⁾. In an attempt to improve or even achieve the agreement with experimental data, various modifications to the original formulation have been proposed, in particular to allow for shell, deformation and pairing effects. However, these models still contain more or less drastic approximations in order to retain the analytical nature of the level density formulation. In particular, simple continuous single particle level densities are adopted. In such models, parameter adjustments overcome the inability of matching known data, mainly the s-neutron resonance spacings at an excitation energy close to the neutron separation energy, which are known for a wide variety of nuclei. However, such a procedure does not at all ensure the correct energy dependence of the predicted level densities. This situation essentially results from the improper treatment of the energy dependence of the shell and pairing corrections.

There have been several attempts to cure these deficiencies, namely on grounds of (i) approximations of the BCS pairing model⁵⁻⁷⁾, (ii) a kind of macroscopic-microscopic approach (e.g. refs.^{8,9)}, and references therein), or (iii) more phenomenological models, like the "constant-temperature" (e.g. ref.³⁾ for references) or "back-shifted" (e.g. ref.¹⁰⁾ for references) level density formulae. All these methods are able to lead to analytical level density formulae containing a certain number of free parameters whose values, determined by comparison with experimental data,

show in particular strong shell, deformation and pairing effects.

In such conditions, the question of the reliability of these methods naturally arises when dealing with nuclei very far from the stability line (sometimes even close to the drip lines), the level densities of which enter as crucial quantities in many problems. Some procedures have been proposed for evaluating the various level density parameters relevant to these nuclei. They essentially rely on known data complemented with the shell and pairing corrections predicted by some mass formulae (e.g. refs.^{11,12)}). It is our opinion that such procedures are rather unsecure, namely in view of the poor quality of the adopted mass formulae. At least, they should have to be confronted with more quantitative studies before being as routinely used as they are very often today.

In fact, many numerical studies already performed in the framework of the partition function method avoid many of the approximations allowed for in order to obtain analytical level density expressions. These calculations have the advantage of retaining the discrete nature of the single particle spectra associated to realistic average potentials. In addition, they can take more properly pairing effects into account. These computations have achieved some success in reproducing experimental data. However, they are not free from difficulties and uncertainties.

One aim of this work is to examine if some of those difficulties can be removed by a different choice of the single particle potentials. The adopted ones are derived in the framework of an energy-density formalism constrained by the requirement of reproducing nuclear binding energies at best (see ref.²⁰⁾, and references therein). In addition, the self-consistent nature of the calculated potentials (at least for spherical nuclei in their ground state), and the ability of the method to predict ground-state properties quite satisfactorily allow us to put some confidence in results concerning nuclei far away from the stability line. Another aim of this paper is to examine the extent to which the pairing treatment can affect the level density predictions, particularly for highly unstable nuclei, and to compare these predictions with those of currently used level density formulae.

Secs. 2 and 3 briefly summarize the basic formulation adopted for the level density calculations, and some properties of the selected single particle and pairing models. Sec. 4 presents a comparison between our level density predictions and experimental data, as well as some results for nuclei very far from the stability line. These latter predictions are confronted with those derived from an analytical level density formula. Some brief conclusions are drawn in Sec. 5.

2. Basic formulation of the level density model

In order to define the notations, and to clearly specify the assumptions made at various stages of the model calculations, we briefly summarize the adopted general formalism (see e.g. refs.^{3,7,13-19)} for more details).

[†]) Chercheur Qualifié F.N.R.S. (Belgium)

2.1 Spherically symmetric systems

2.1.1 General formalism. We first consider spherically symmetric nuclei with N neutrons, Z protons, projection M of the total angular momentum, and energy E , corresponding to an excitation energy $E^* = E - E_0$, E_0 being the ground state energy (other first integrals of motion have also been considered, like the isospin; see e.g. ref.²¹). The neutron and proton systems are always assumed to be in thermodynamical equilibrium, and any residual quasineutron-quasi-proton interaction²⁹) is neglected.

If each nucleon system is described in terms of the usual BCS hamiltonian (see e.g. ref.²²), its thermodynamical behavior can be described by the logarithm Ω of its grand partition function, given by¹³⁻¹⁶)

$$\Omega = -\beta \sum_{\kappa} (\epsilon_{\kappa} - \lambda - E_{\kappa}) + \sum_{\xi=\pm 1} \sum_{\kappa} \ln\{1 + \exp(-\beta(E_{\kappa} + \xi \gamma m_{\kappa}))\} - \beta \sum_{\kappa \kappa'} G_{\kappa \kappa'} \chi_{\kappa} \chi_{\kappa'} \quad (1)$$

where β , $\lambda = \alpha/\beta$, and $\gamma = \mu/\beta$ are the Lagrange multipliers which fix the energy, the particle number, and the angular momentum projection, respectively. The parameter β is also the reciprocal of the thermodynamical temperature t , while λ is identified with the chemical potential. Note that the neutron and proton systems have the same β and γ values. On the other hand, m_{κ} is the spin projection (defined positive) of the κ -th doubly degenerate single particle level with energy ϵ_{κ} (assumed to be temperature independent),

$$E_{\kappa} = \{(\epsilon_{\kappa} - \lambda)^2 + \Delta_{\kappa}^2\}^{1/2} \quad (2)$$

being the corresponding quasiparticle energy. In this expression, Δ_{κ} is the gap parameter, solution of the gap equation

$$\Delta_{\kappa} = \sum_{\kappa'} G_{\kappa \kappa'} \chi_{\kappa'} \quad (3)$$

where

$$\chi_{\kappa} = \sum_{\xi=\pm 1} \Delta_{\kappa} \operatorname{tgh}\{\beta(E_{\kappa} + \xi \gamma m_{\kappa})/2\} / (4E_{\kappa}) \quad (4)$$

In Eqs. (1) and (3), $G_{\kappa \kappa'}$ is the pairing matrix element which measures the strength of the pairing interaction between the levels κ and κ' . Note that Eqs. (1)-(4) explicitly exclude blocking effects, which will always be neglected in nuclear excited states.

At an excitation energy E^* , a spherical nucleus with N neutrons and Z protons has a density $\rho(E^*, N, Z, M)$ of intrinsic levels with angular momentum M . That density is given by the inverse Laplace transform of the total grand partition function $\Omega = \Omega_n + \Omega_p$, where $\Omega_n(p)$ refers to the neutron (proton) system only, and is expressed by Eq. (1). This transform leads to a Darwin-Fowler integral which can be evaluated with a satisfactory approximation by means of the saddle-point technique, except in particular for certain low excitation energies (see e.g. ref.²³). This approximation leads to the classical result¹)

$$\rho(E^*, M) = \exp(S) / \{(2\pi)^4 D\}^{1/2} \quad (5)$$

where $S = S_n + S_p$ is the total entropy of the system, while D is the 4×4 determinant of the second derivatives of Ω with respect to the Lagrange multipliers involved in the problem. For use in Eq. (5), S and D have to be evaluated at the saddle point defined by

$$N = \partial\Omega/\partial\alpha_n; \quad Z = \partial\Omega/\partial\alpha_p; \quad M = \partial\Omega/\partial\mu; \quad E^* = \partial\Omega/\partial\beta - E_0 \quad (6)$$

where $\alpha_n(p)$ is the α multiplier for the neutron (pro-

[†]) Here and in the following, N and Z are not mentioned explicitly anymore in the list of arguments of the level density

ton) system defined in connection with Eq. (1). The explicit expressions for S and D , as well as for the quantities appearing in Eq. (6) can be found in e.g. refs.¹³⁻¹⁶).

On the other hand, the BCS ground-state energy E_0 in Eq. (6) can be easily evaluated from the $t = 0$ limit of Eq. (3), $E = \partial\Omega/\partial\beta$, and Eq. (6) for N and Z . Blocking is traditionally neglected in the calculation of E_0 for use in level density estimates, the quasiparticle approximation (Sec. 2.1.7) being adopted instead when dealing with odd- N and/or odd- Z nuclei. This approximation can, however, be rather easily avoided. The explicit form of the corresponding ground-state equations can be found in e.g. ref.²⁴) (see also Sec. 2.1.6).

The solution of the system of Eqs. (3) and (6) provides the values of all the required unknowns for the calculation of Eq. (5) for given N , Z , E^* and M once the pairing matrix and single particle spectrum are known for the neutron and proton systems. In practice, and especially in the framework of realistic single particle spectra and pairing models, the solution of this problem is far from being trivial, and prohibitively time consuming when dealing with many nuclei and/or large excitation energy ranges. This is the reason why various levels of approximation have been considered. Before describing them briefly (Secs. 2.1.4-6), let us, however, make some remarks.

2.1.2 Nuclear phase transition. An interesting property of the above mentioned system of equations is that all the Δ_{κ} 's go to zero at some critical temperature t_{cr} for each nucleon system. This temperature only depends upon the angular momentum, and can in fact be zero for high enough values of this momentum. This property has been discussed in some detail in e.g. ref.¹⁵). At such a critical point, a second order phase transition from the paired to the unpaired regime occurs, and translates into a discontinuity of the determinant D (Eq.(5)). Such a sharp phase transition is probably spurious in nuclear systems, which are expected to exhibit large fluctuations, namely in the Δ_{κ} 's, and may be avoided by the use of average quantities rather than the most probable values derived from the solution of the above mentioned system of equations¹⁵). No attempt will be made in the following to introduce such a correction.

2.1.3 Continuum corrections. Various of the equations of Sec. 2.1 involve summations over the eigenstates of a single particle potential. Normally, no divergent behavior of those summations is expected when using infinite potentials, at least if the matrix elements $G_{\kappa \kappa'}$ exhibit the well-known feature of decreasing with increasing energies $\epsilon_{\kappa \kappa'}$. In practice, however, the required single particle basis may be too large to handle, so that some truncation procedure is normally applied.

In finite potentials, somewhat different summation problems arise. In particular, at high enough temperatures and/or for nuclei far away from the stability line, single particle states farther away from the Fermi energy than the binding energy of the last nucleon may contribute significantly. This problem can be handled²⁵) by replacing in the $\epsilon > 0$ region the various summations by integrals over a continuum single particle state density related to the derivatives of scattering phases with respect to ϵ ²⁶). As these derivatives may be positive or negative, some cancellation of the bound state contribution by continuum scattering states is possible. This cancellation is in fact complete in the limit of infinite temperatures.

In most calculations, however, the phase shift analysis is avoided by a discretization of the continuum into "quasibound" states. The smallness of the $G_{\kappa \kappa'}$'s and Δ_{κ} 's for these levels provides a natural

cut-off in the equations which contain summations involving pairing quantities. However, several criticisms can be made about this technique^{25,27}), which cannot be fully trusted in particular when a substantial fraction of the nucleons can be excited in the $\epsilon > 0$ region.

2.1.4 The spin- and parity-dependent level densities. The analysis of experimental data often requires the prediction of the density of levels of a given spin I and/or parity π . As suggested by Bethe¹), $\rho(E^*, I)$ can be evaluated from

$$\rho(E^*, I) = \rho(E^*, M) - \rho(E^*, M+1). \quad (7)$$

On the other hand, the statistical methods described up to now are normally not able to provide very reliable parity distributions. An approximate method has been proposed²) which, in fact, shows that both parities become rapidly almost equally probable with increasing excitation energies. On such grounds, it is usually assumed that

$$\rho(E^*, I, \pi) = \rho(E^*, I)/2 \quad (8)$$

for any excitation energy.

From $\rho(E^*, I)$, various other quantities of interest can be derived, like the observable level density

$$\rho_{\text{obs}}(E^*) = \sum_I \rho(E^*, I), \quad (9)$$

the state density (sometimes also referred to as the total level density)

$$\omega(E^*) = \sum_I (2I+1) \rho(E^*, I), \quad (10)$$

or the s-neutron resonance spacing

$$D = f_{\pi} \{ \rho(E^*, I_0 - 1/2) + \rho(E^*, I_0 + 1/2) \}^{-1}, \quad (11)$$

where f_{π}^{-1} is the probability of having resonances of the required parity ($f_{\pi} = 2$ in the approximation of Eq. (8)), and I_0 is the target spin (only the second density in Eq. (11) is relevant if $I_0 = 0$).

2.1.5 The spin-independent pairing approximation
In most level density calculations based on the partition function method and on the BCS approximation, M is generally not included from the start as a first integral of motion. This reduces to three the number of Lagrange multipliers, and the problem can be simply reformulated by putting $\gamma = 0$ in the general equations. In such conditions, the pairing correlation becomes independent of the angular momentum, as are in particular $t_{\text{cm}, p}$ (Sec. 2.1.2). In this approximation, the equivalent of Eq. (5) gives the state density

$$\omega(E^*) = \exp(S) / \{ (2\pi)^3 D \}^{1/2}. \quad (12)$$

The level density $\rho(E^*, M)$ is then obtained from this equation by assuming¹) that the nucleus spin projections on the quantization axis have a gaussian distribution with an average value of zero, and a mean square deviation¹³⁻¹⁵)

$$\sigma^2 = \frac{1}{2} \sum_{\kappa} \epsilon_{\kappa}^2 \text{sech}^2(\beta E_{\kappa} / 2), \quad (13)$$

σ being classically referred to as the spin cut-off parameter. In such conditions,

$$\rho(E^*, M) = \omega(E^*) \exp(-M^2 / 2\sigma^2) / (2\pi\sigma^2)^{1/2}, \quad (14)$$

which, through the use of Eq. (7), leads to the well-known expression

$$\rho(E^*, I) = \omega(E^*) (2I+1) \exp\{-I(I+1) / 2\sigma^2\} / \{ 2(2\pi)^{1/2} \sigma^3 \}, \quad (15)$$

The validity of the spin cut-off approximation has been discussed in several places (see e.g. refs. 15, 28)). In brief, such an approximation appears to be the poorest at rather low temperatures and high angular momenta. These are just the conditions in which the angular momentum plays a key role in the pairing properties. This question is very briefly reexamined in Sec. 4.3.

2.1.6 The constant-G approximation. In many calculations based upon the BCS approximation, it is generally assumed that the pairing matrix elements of greatest relevance (i.e. those involving single particle levels in the vicinity of the Fermi surface) are equal to some constant G , referred to in the following as the pairing strength constant. The level density calculations then greatly simplify, as the system of Eqs. (3) is replaced by the single gap equation

$$2/G = \sum_{\kappa} \sum_{\epsilon} \text{tgh}\{\beta(E_{\kappa} + \epsilon \gamma m_{\kappa}) / 2\} / (2E_{\kappa}). \quad (16)$$

When used in conjunction with infinite single particle potentials, Eq. (16) is, however, diverging. In order to avoid this, and to obtain results in agreement with experiment, the constant-G approximation thus requires some suitable truncation of the shell model space, and a renormalization of G . The most usual truncation procedures involve the consideration of a suitable energy range, or of a given number of single particle levels around the Fermi surface.

The values of the pairing strength constants can then be evaluated on grounds of "experimental" odd-even mass differences $P_{n,p}$. The extraction of such quantities from known data is, however, far from being trivial, as the contamination by parasitical (e.g. shell or deformation) effects is not easy to avoid. Among the various existing prescriptions for evaluating $P_{n,p}$ (see e.g. ref. 23)), the one proposed by Beiner appears able to minimize these contamination effects²⁹). The derived $P_{n,p}$ values (which are sometimes approximated by smooth values close to $12A^{-1/2}$, A being the mass number) then serve to calculate $G_{n,p}$ through a condensation energy computation³⁰).

2.1.7 The quasiparticle approximation (QPA).
The condensation energy method allows the evaluation of $G_{n,p}$ with due consideration of blocking effects, but is numerically less attractive than a commonly used approximation which neglects blocking, and relies on the identification

$$P = E_1 = \{ (\epsilon_1 - \lambda)^2 + \Delta^2 \}^{1/2} \quad (17)$$

for each nucleon system, ϵ_1 being the energy of the last occupied single particle level. This equation, used in conjunction with the $t=0$ limit of the particle number equation (6), can provide the G value through the $t=0$ limit of Eq. (16). The validity and limitations of this approximate treatment (referred to as QPA) have been discussed in several places in the literature (see e.g. ref. 24)).

The QPA applied to an ensemble of nuclei with known $P_{n,p}$ leads to $G_{n,p}$ values which do not exhibit strong deviations from a smooth trend. This gives some support to a commonly used approximation of pairing strength constants varying smoothly with the particle number.

In the spirit of the QPA, the state densities of nuclei with odd- N and/or odd- Z are very often evaluated from (see e.g. ref. 17))

$$\omega_{ee}(E^*) = \omega_{oe}(E^* - E_{1n}) = \omega_{eo}(E^* - E_{1p}) = \omega_{oo}(E^* - E_{1n} - E_{1p}), \quad (18)$$

where the first and second subscripts $e(o)$ refer to even(odd) neutron and proton numbers, respectively, while $E_{1n,p}$ is given by Eq. (17).

2.1.8 Contribution of vibrational states. The various level density expressions given up to now uniquely refer to intrinsic states. The inclusion of collective vibrational modes in level density models for spherical nuclei has been considered in e.g. ref.³¹). These considerations may also be extended to deformed nuclei (Sec. 2.2). However, the contribution of vibrational states is neglected in all the calculations to be reported below, and will be studied elsewhere.

2.2 Extension of the level density model to statically deformed nuclei

2.2.1 General formalism. In deformed nuclei, the occurrence of collective rotational motion leads to an increase of the nuclear level densities^{7,17,19,31}). Assuming axial symmetry, and the existence of a rotational band on top of each intrinsic state with quantum number K (component of I along the symmetry axis), the level density $\rho(E^*, I)$ can be evaluated from

$$\rho(E^*, I) = \frac{1}{2} \sum_{K=-I}^{+I} \rho_{\text{intr}}(E^* - E_{\text{rot}}(K, I), K), \quad (19)$$

where the intrinsic level density ρ_{intr} can be evaluated as described in Sec. 2.1, K and Ω_K (projection of the single particle angular momentum on the symmetry axis) having to replace M and m_K , respectively. In Eq. (19), the rotational energy

$$E_{\text{rot}}(K, I) = \frac{\hbar^2}{2J_{\perp}} \{I(I+1) - K^2\} \quad (20)$$

can be evaluated if the moment of inertia J_{\perp} associated to the collective rotation about an axis perpendicular to the symmetry axis is known. An energy dependent J_{\perp} can be computed from (ref.³²), Eq. (4.128))

$$J_{\perp} = \frac{2}{5} M_{\text{u}} R^2 (1 + \frac{1}{3} \delta) \{N \{1 - g \frac{\delta \hbar \omega_0}{2 \Delta_n}\} + Z \{1 - g \frac{\delta \hbar \omega_0}{2 \Delta_p}\}\}, \quad (21)$$

where M_{u} is the atomic mass unit, R the mean nuclear radius, δ a deformation parameter (defined as in ref.³²), $\hbar \omega_0 = 41 A^{-1/3}$, $\Delta_{n,p}$ the spin-independent pairing correlation functions (Sec. 2.1.5), and

$$g(x) = \ln\{x + (1+x^2)^{1/2}\} \{x^2(1+x^2)\}^{-1/2}. \quad (22)$$

We have verified that Eq. (21) is able to predict ground state J_{\perp} values which are in general within 20% of the experimental ones.

The validity of the approximations leading to Eq. (19) has been discussed in e.g. ref.³¹). It is namely concluded that the separation of the rotational and intrinsic degrees of freedom remains valid up to temperatures of the order of $\delta \hbar \omega_0$. At higher temperatures, the expression (see e.g. ref.¹⁷))

$$\rho_{\text{ht}}(E^*, I) \approx (2I+1) \rho_{\text{intr}}(E^*, K=I+\frac{1}{2}) / (2\sigma^2) \quad (23)$$

is expected to provide a more realistic estimate of the level densities, ρ_{intr} being evaluated from e.g. Eq. (14). A closely connected question concerns the energy dependence of the nuclear deformation. In most level density calculations performed up to now, the ground state deformation is adopted at all energies. The validity of such an approximation remains to be examined in detail. The question of the departure from axial symmetry, and of the vibrational contribution (Sec. 2.1.8) may also be of interest (e.g. ref.³¹).

2.2.2 Pairing strengths for deformed nuclei.

The evaluation of the pairing matrix for deformed nuclei requires a substantial amount of computer time, so that the constant-G approximation (Sec. 2.1.6) is particularly useful in these cases. The possibility of

some dependence of the pairing strength upon deformation has been raised several times. However, as discussed in e.g. ref.³³), the situation is still far from being clear.

3. The adopted single particle model and pairing strengths

The single particle properties (spectrum, deformation) required for the level density calculations are derived from an energy-density formalism described in detail elsewhere²⁰). Let us simply emphasize some points of special relevance or importance in the level density context:

(i) the ground state single particle potentials for spherical or quasi-spherical nuclei are derived in a self-consistent way under the requirement of reproducing nuclear binding energies at best. Deformed potentials are not fully self-consistent, and are obtained by deforming self-consistent spherical ones;

(ii) the ability of the method to reproduce various ground state properties quite satisfactorily, and its self-consistent or "close to self-consistent" nature allow us to put some confidence in extrapolations far from the line of nuclear stability. In these regions, the adopted model makes several predictions which might have important consequences on the level density estimates. In particular, the sequence of magic numbers and/or the degrees of magicity may depend upon the distance from the stability line;

(iii) several sets of calculations have been performed with different choices of the pairing strengths. In one case, the pairing strength constants are evaluated from the QPA and Beiner's prescription for estimating $P_{n,p}$ (Secs. 2.1.6,7). Such calculations include all bound single particle levels and suitably chosen quasibound states up to $2\hbar\omega_0$. Smooth $G_{n,p}$ values parametrized as

$$G_n = 2.25/N^{0.7}; \quad G_p = 2.00/Z^{0.7} \quad (24)$$

are proposed from these computations. In another case, the same single particle levels are used to calculate pairing matrices on grounds of a δ -interaction model, the single pairing parameter encountered in this case being selected in order to fit $P_{n,p}$ at best;

(iv) average pairing constants $\langle G_{n,p} \rangle$ defined from the pairing matrices show rather substantial deviations from the behavior (24) far from the stability line³³). In addition, strong deviations of the odd-even mass differences from the empirical $P_{n,p} \propto A^{-1/2}$ are also encountered far from stability.

4. Some results

4.1 The s-neutron resonance spacings

These quantities are known for a wide variety of nuclei at an excitation energy close to the neutron separation energy. This large body of informations is compared to predictions of the level spacing D (Eq. 11)) using the constant-G approximation (Sec. 2.1.6) in conjunction with the spin-independent pairing approximation (Sec. 2.1.5). Fig. 1 presents such a comparison, the $G_{n,p}$ values being derived from the QPA and Beiner's method for the extraction of $P_{n,p}$, while $f=2$ is used in Eq. (11). All the displayed $180 < A < 200$ nuclei are assumed to be deformed, and their level densities, as well as those of the rare earths and actinides, are evaluated from Eqs. (19)-(22). The calculational procedure adopted for constructing Fig. 1 is referred to as the standard prescription in the following.

In absence of any fitting to level density data, the standard calculations achieve an overall fair agreement with experiment. This is especially the case

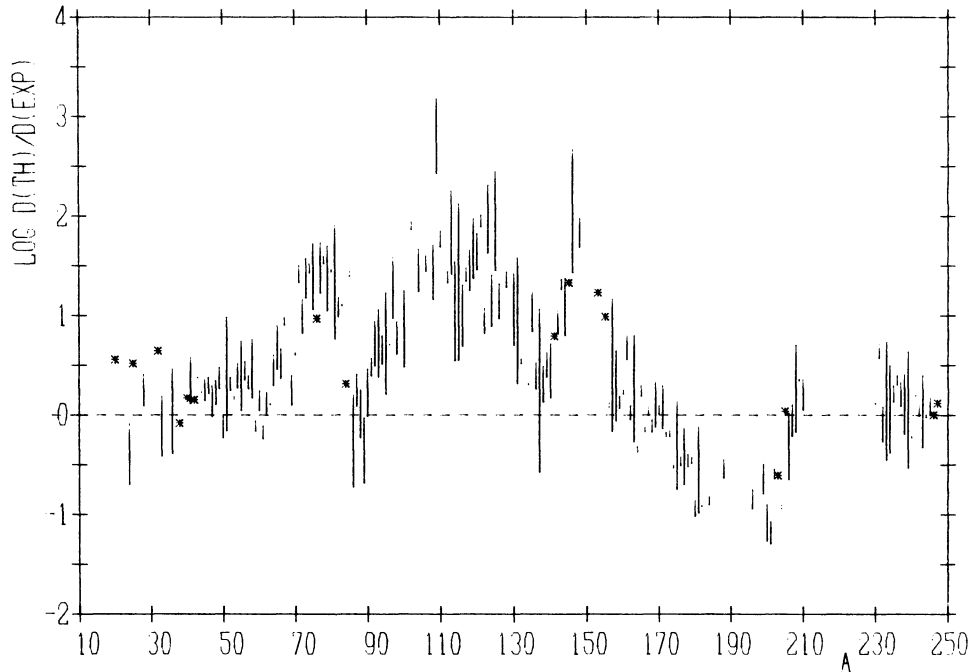


Fig. 1 Comparison between theoretical $D(TH)$ and experimental $D(EXP)$ values of the s -neutron resonance spacings at an excitation energy equal to the neutron separation energy. The experimental data are taken from several compilations³⁹⁻⁴¹, while the calculations are done with the standard set of assumptions defined in the main text. The vertical bar for a given A represents the range of $D(TH)/D(EXP)$ values derived for several isobars and/or several experimental data. For clarity, symbols $*$ are used in place of very small vertical bars

in the $A \lesssim 70$ region, in the vicinity of various magic nucleon numbers (note in particular the very good agreement at $A=208$), as well as in the rare earth and actinide regions. However, some deviations and systematic structures are also observed. In order to examine the extent to which these features may depend upon some particular ingredients of the standard prescription, some other sets of computations have been performed. In particular,

(i) Ericson's² prescription is used in order to evaluate f (Eq. (11)). Except in some specific cases (especially with $A \lesssim 50-60$), the derived values at the relevant excitation energies are very close to $f=2$ used in the standard case. Thus, the general pattern of Fig. 1 remains unchanged;

(ii) instead of the experimentally derived $G_{n,p}$ values, Eq. (24) is used. The corresponding level spacings are globally the same as those of Fig. 1. Of course, this is not surprising, as Eq. (24) represents a smooth fit to the "experimental" $G_{n,p}$'s. However, some slight and systematic differences are noticed in certain mass regions, like in the $70 \lesssim A \lesssim 80$ and $150 \lesssim A \lesssim 190$ ranges, where the standard results are somewhat less satisfactory, while the reverse holds for the actinides;

(iii) in order to analyse the sensitivity of the level density results to the underlying single particle potential models, D for spherical nuclei have also been calculated using a Woods-Saxon potential tailored for providing a high-quality fit to the single particle spectra of the doubly closed shell nuclei from 160 to ^{208}Pb ³⁴). The corresponding D values agree remarkably with those of Fig. 1. These latter results also agree with, but are however systematically somewhat lower than the D values calculated with a Woods-Saxon potential whose parameters are evaluated on grounds of a Thomas-Fermi approximation¹⁷) (it is, however, somewhat dangerous to assign these differences to the

adopted single particle spectra only, as several other features of the two models are different). Ordinary Nilsson and folded Yukawa potentials have also been used in certain level density calculations (see e.g. ref.¹⁷) for references and some comparison between the various derived level densities);

(iv) a limited number (due to the required computer time) of calculations have also been performed with the δ -interaction matrix mentioned previously, and compared with the results of set (ii). The derived densities are very similar (see also ref.¹⁶)).

Let us now briefly discuss some of the main discrepancies between theory and experiment which show up in Fig. 1.

4.1.1 The $70 \lesssim A \lesssim 85$ range. Our calculated level densities for those nuclei are too low by factors $\sim 20-30$. In a search for the origin of such a discrepancy, some computations have been performed with the slightly deformed single particle potentials predicted by the adopted energy density formalism. The full contribution of the rotational bands helps reducing the predicted D 's by an average factor of the order of 10. However, such an inclusion may not be totally justified, as the temperatures at the excitation energies of interest are not much smaller than $\delta^* \omega_0$ (Sec. 2.2). On the other hand, Eq. (23) leads to results which are very close to the spherical ones;

4.1.2 The $100 \lesssim A \lesssim 130$ range. Deformation effects have been proposed as a solution to this classical puzzle in level density calculations (see e.g. refs. 17,35)). Our calculations indeed confirm that some of those nuclei might have ground state deformations. For example, $\delta=0.15$ is found for nuclei like ^{110}Pd or ^{126}Xe . If the full rotational contribution is taken into account, the corresponding D 's are reduced by $\sim 10-100$ in the $E^* < 10$ MeV range, for which $t < \delta^* \omega_0$. However, some of the nuclei in the considered

range (and in particular Sn) do not have significant ground state deformations. In such cases, a reduction of D might result from the existence of a significant number of deformed intrinsic states at excitation energies close to the neutron separation energy. Some calculations performed in the formalism of Sec. 3 do not contradict this possibility, and we are planning to investigate such a question in greater detail. Let us finally note that a decrease of D by a factor ~ 100 can be achieved in the spherical case if, in that mass region, the standard pairing strengths are reduced by about 20%. However, there is no a priori reason justifying such a reduction. It may also be of interest to mention that this mass region is especially difficult to handle experimentally;

4.1.3 The $190 \leq A \leq 200$ range. The formalism of Sec. 3 predicts slightly deformed nuclei in that region. When the contribution of the rotational bands is taken into account, the corresponding level spacings appear to be smaller than the experimental data. In view of the uncertainties in the derived single particle potentials in that mass range, some calculations have also been performed with a built-in spherical symmetry. The corresponding D 's essentially agree with the previous results. As the condition $t \ll \delta t \omega_0$ is not necessarily satisfied at the relevant excitation energies, use has also been made of Eq. (23). The resulting D 's are about 10 times larger than the experimental ones. Note that this is in contrast with the situation encountered in Sec. 4.1.1, where the spherical results are in close general agreement with those of Eq. (23).

In summary, the predicted D 's are very sensitive to deformation and/or to the exact contribution of the rotational bands in the mass regions of highest discrepancy between theory and experiment. In order to clarify the problem, a further detailed study appears necessary, including in particular some energy dependence of the deformation, the contribution of vibrational states, or even other residual interactions (e.g. quadrupole pairing³⁶).

4.2 The energy dependence of the level densities

A much smaller amount of reliable experimental data are available concerning the energy dependence of the level densities than about the resonance spacings at an excitation energy close to the neutron separation energy.

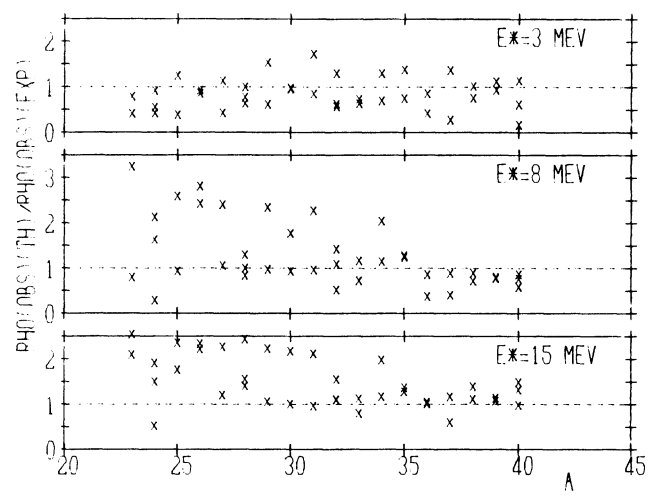


Fig. 2 Comparison between the observable level densities calculated from Eq. (9) on grounds of our standard set of assumptions (denoted $\rho_{\text{OBS}}(\text{TH})$ in the figure), and the corresponding values derived from experiment³⁷ (denoted $\rho_{\text{OBS}}(\text{EXP})$). The comparison is performed for three excitation energies E^*

Such an energy dependence has been examined in some detail for $A \leq 40$ nuclei³⁷), and some of these data at 3 excitation energies are compared in Fig. 2 to our predictions based on the standard set of assumptions defined in Sec. 4.1. At $E^* = 3$ MeV, most of the considered nuclei are still in the paired regime, the reverse being true at $E^* = 15$ MeV. It appears that a quite fair agreement with the experimental data is achieved at all the considered E^* , even if relatively light nuclei are involved. The energy dependence of the level densities thus appears to be quite satisfactorily predicted on grounds of our standard set of assumptions. This energy dependence is also quite similar to the one calculated with the δ -interaction pairing matrix.

4.3 Validity of the spin cut-off approximation

Some computations of the observable level densities have also been performed without the aid of the spin cut-off approximation (see Eq. (15)). However, in view of the required computer time, only about 10 of the nuclei displayed in Fig. 2 have been considered at $E^* = 3$ MeV. The results obtained in such a way are within a factor of about 2-3 of those obtained in the standard calculations. Some additional computations performed in a more extended energy range and for heavier nuclei confirm this result. It thus appears likely that the spin cut-off approximation is quite satisfactory in the energy and angular momentum conditions of relevance in the construction of Fig. 2, as well as of Fig. 1. This question has also been examined in detail by Døssing²⁸), particularly at higher energies and angular momenta.

4.4 Level densities of nuclei far from stability

In order to examine the influence on the level densities of variations in the characteristics of the single particle spectra and pairing correlations when going away from the stability line (Sec. 3), some preliminary and exploratory calculations have been performed for the $N=60$ and $N=126$ isotonic chains between the neutron and proton drip lines. All these nuclei are assumed to be spherical.

The level densities predicted for some of these nuclei with the δ -interaction pairing matrix and with the constant pairing strengths of Eq. (24) are compared in Fig. 3 for several excitation energies. While the two methods give rather similar results in the vicinity of the stability line (note, however, some shell effect structure around the $Z=50$ and 82 magic numbers), they have a tendency to exhibit larger deviations further away from the stability line, the level densities calculated with the pairing matrix being higher than those resulting from the use of Eq. (24), particularly for very neutron-rich species at relatively high excitation energies. This trend has not been studied in detail up to now. However, and at least for $N=60$, it might result from the increasing role of quasibound states in the above mentioned conditions. The pairing matrix elements involving such levels being lower than those associated to bound states, some reduction of the effective pairing strengths may result, accompanied with a level density increase. Of course, Eq. (24) cannot account for this effect. In the more neutron deficient region, only protons quasibound states can play a role in the considered conditions, and the trend is less clear. This is probably due to the fact that the effective pairing strength reduction associated to those levels is less severe than for neutrons³³). The $N=126$ case cannot be totally accounted for in such a way.

The use of pairing matrices is thus recommended when dealing with nuclei far from the stability line. Of course, in view of the uncertainties which may affect the quasibound level approach (Sec. 2.1.3), it would be desirable to perform some phase shift analy-

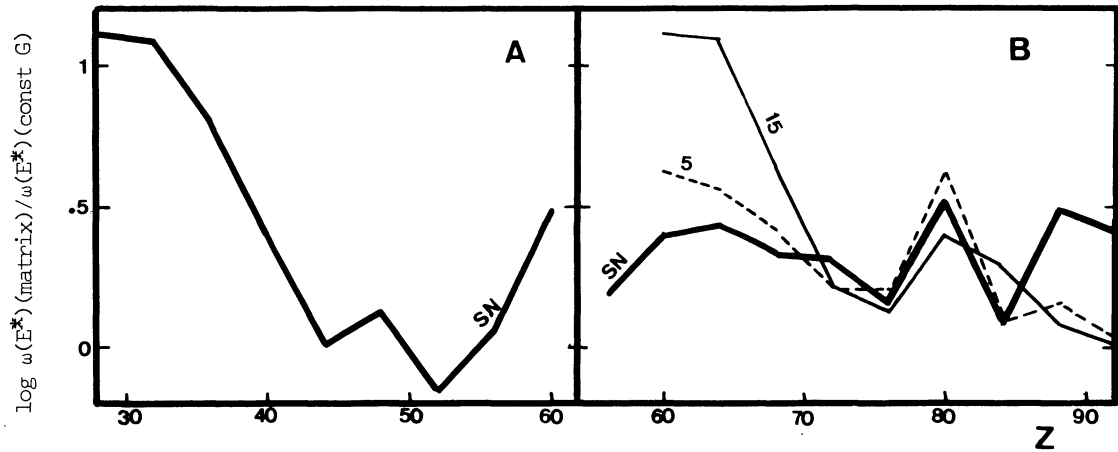


Fig. 3 Comparison between the state densities $\omega(E^*)$ (Eq. (12)) evaluated on grounds of the δ -interaction pairing matrix (denoted $\omega(E^*)(\text{matrix})$), and those derived from the G values given by Eq. (24) (denoted $\omega(E^*)(\text{const G})$). This comparison is performed for two isotonic chains (N=60 in part A, and N=126 in part B), and for several excitation energies whose values (in MeV) label the curves (SN symbolizes the neutron separation energy)

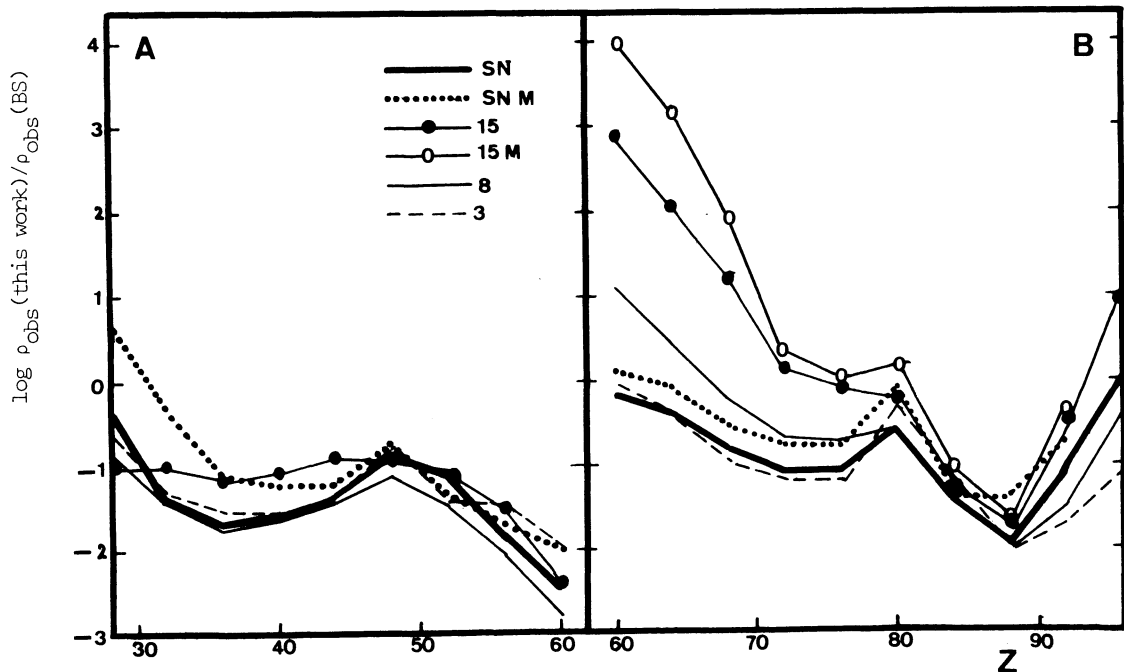


Fig. 4 Comparison between the observable level densities calculated from Eq. (9) (denoted $\rho_{\text{obs}}(\text{this work})$), and those derived from a back-shifted Fermi gas model¹² (denoted $\rho_{\text{obs}}(\text{BS})$). The values $\rho_{\text{obs}}(\text{this work})$ are evaluated either with the δ -interaction pairing matrix (curves labelled M), or on grounds of the G values given by Eq. (24). The comparison is performed for the chains N=60 (part A) and N=126 (part B), as well as for several energies whose values (in MeV) are indicated in the figure (SN symbolizes the neutron separation energy)

sis before drawing firm conclusions.

4.5 Comparison with other level density models

Fig. 4 compares the level density results used in the construction of Fig. 3 to the predictions of a back-shifted Fermi gas model¹² (referred to as BSFG in the following). It namely appears that, in the N=126 case, the two models agree fairly well in the explored energy range ($3 \leq E^* \leq 15$ MeV) close to the stability line (let us remind that the BSFG model is fitted to experimental data in that region). When moving away from the stability line, more and more pro-

nounced differences appear, their extent depending upon the degree of neutron enrichment or deficiency, as well as upon excitation energy. In particular, the two sets of results may differ by factors ≥ 100 relatively close to the neutron drip line, and at $E^* > 10$ MeV. Of course, in those conditions, further calculations have to be performed in order to check the validity of our quasibound level treatment.

In the N=60 case, our results slightly underestimate the level densities around the stability line (Fig. 1). Taking this reservation in mind, diverging trends also appear between our calculations and the

BSFG predictions, particularly in the neutron-deficient region. On the neutron-rich side, the situation is somewhat less clear.

The divergences between the two sets of predictions are likely due to differences in the treatment of the shell and pairing effects. In particular, the BSFG model under consideration makes use of smooth single particle level densities, and of energy-independent level density parameters a (Sec. 4.6). Furthermore, the adopted shell and pairing corrections are derived from a rather low-quality mass formula. Of course, further and more systematic calculations (involving also deformed nuclei) are required in order to draw more detailed conclusions about the differences between our calculations and the predictions of other models very far from the stability line.

4.6 The level density parameter a

In the simplest and most widely used level density formulations, the entropy S is simply related to the temperature through $S = 2at$, a being commonly referred to as the level density parameter.

This parameter plays a pivotal role in the level density estimate (see Eqs. (5),(12)), and is classically related to the single particle level density at the Fermi surface. In the vast majority of analytical level density formulae, a is considered to be energy independent. Many such models for a have been proposed recently in the literature, relying in particular on Thomas-Fermi approximations³⁸), or on microscopic-macroscopic methods inspired from techniques developed for predicting nuclear masses (see e.g. ref.⁹), and references therein). Such models provide formulae for the smooth part of a (excluding shell effects) which contain in particular volume, surface and curvature terms³⁸). An isospin and shape dependence of a has also been considered in such frameworks, and a dependence upon the last neutron and proton separation energies has been stressed as well⁹).

Several of these predictions have been compared to our results. At low enough temperatures, our calculations show a more or less pronounced energy dependence of a which cannot be accounted for by the above mentioned simple models. When these effects (essentially associated to shell and pairing energy dependence) die out, our predicted a 's can be more directly compared with the simple model results. We find "asymptotic" a values in the ranges $0.10 \leq a/A \leq 0.11$ and $0.095 \leq a/A \leq 0.10$ for the $N=60$ and $N=126$ isotones of Figs. 3,4, respectively. These values agree to within $\leq 10\%$ with those derived in ref.³⁸) (when use is made of the S-VI effective interaction), but diverge more strongly with those proposed in ref.⁹). In addition, our results do not confirm the relation between a and the last neutron and proton separation energies put forth in this latter work. We are planning to perform more systematic calculations in order to examine this question in greater detail.

5. Conclusions

The level density model presented in this paper is considered to constitute an interesting tool for predicting nuclear level densities, particularly at relatively low excitation energies, and far from the line of β -stability. Certain remaining difficulties, however, emphasize the need for some further improvements.

In fact, limitations of various natures affect the model. On the statistical side, a minor shortcoming is expected to arise from the use of (i) the saddle point approximation, at least at very low temperatures, (ii) the spin cut-off approximation, at least at low energies and very high angular momenta, and (iii) most probable instead of average quantities,

this being responsible for the spurious phase transition at the critical temperatures.

On the nuclear side, it would be of interest to (i) construct self-consistent finite temperature single particle potentials, (ii) examine in greater detail the influence of the associated nucleon effective masses and of their energy dependence on the level density predictions³⁸), and (iii) try including other residual interactions than those considered in this work. In view of the high sensitivity of certain predicted level densities on the pairing characteristics, a more careful evaluation of the pairing strengths based namely on the condensation energy method rather than on the QPA would also be desirable. The study of a possible nuclear shape dependence of the pairing strengths would also have to be pursued. In this connection, a more careful examination of the contribution of rotational and vibrational collective states appears necessary. This problem is intimately related to the question of the possible energy dependence of the nuclear deformation. Finally, let us remind that the role of the continuum on the level density predictions has to be carefully examined, particularly when dealing with nuclei close to the drip lines and/or high excitation energies. We are planning to examine some of those questions in a near future.

Acknowledgments. One of the authors (M.A.) gratefully acknowledges the hospitality of the Institut für Kernphysik of the Technische Hochschule Darmstadt, where part of this work has been done. In this respect, he is particularly indebted to E. Hilf and K. Takahashi. He also thanks the Alexander von Humboldt Stiftung, the Gesellschaft für Schwerionenforschung (GSI) Darmstadt, and the Deutsche Forschungsgemeinschaft (DFG) for their partial financial support.

References

1. H. A. Bethe, Phys. Rev. **50**:332 (1936); Rev. Mod. Phys. **9**:69 (1937).
2. T. Ericson, Advan. Phys. **9**:425 (1960).
3. J. R. Huizenga and L. G. Moretto, Ann. Rev. Nucl. Sci. **22**:427 (1972).
4. V. S. Stavinskii, Sov. J. Part. Nucl. **3**:417 (1973).
5. M. Sano and S. Yamasaki, Prog. Theor. Phys. **29**:397 (1963).
6. T. Kammuri, Prog. Theor. Phys. **31**:595 (1964).
7. M. Sano and M. Wakai, Prog. Theor. Phys. **48**:160 (1972).
8. A. S. Jensen and J. Sandberg, Phys. Scripta **17**:107 (1978).
9. S. K. Kataria and V. S. Ramamurthy, Nucl. Phys. **A349**:10 (1980).
10. A. N. Behkami and J. R. Huizenga, Nucl. Phys. **A217**:78 (1973).
11. A. Gilbert and A. G. W. Cameron, Can. J. Phys. **43**:1446 (1965).
12. J. A. Holmes, S. E. Woosley, W. A. Fowler and B. A. Zimmerman, Atomic Data Nucl. Data Tables **18**:305 (1976).
13. L. G. Moretto, Nucl. Phys. **A182**:641 (1972).
14. L. G. Moretto, Nucl. Phys. **A185**:145 (1972).
15. L. G. Moretto, Nucl. Phys. **A226**:9 (1974).
16. L. G. Moretto and S. K. Kataria, Nuovo Cim. **9**(ser. 2):190 (1974).
17. T. Døssing and A. S. Jensen, Nucl. Phys. **A222**:493 (1974).
18. J. R. Huizenga, A. N. Behkami, J. S. Svntek and R. W. Atcher, Nucl. Phys. **A223**:577 (1974).
19. J. R. Huizenga, A. N. Behkami, R. W. Atcher, J. S. Svntek, H. C. Britt and H. Freiesleben, Nucl. Phys. **A223**:589 (1974).
20. F. Tondeur, This Conference.

21. A. S. Jensen, Phys. Letters 68B:105 (1977).
22. J. M. Eisenberg and W. Greiner, Nuclear Theory Vol. 3 (North-Holland Pub. Co.; Amsterdam), p. 287 (1972).
23. A. Bohr and B. R. Mottelson, Nuclear Structure Vol. 1 (Benjamin; New York) (1969).
24. S. Wahlborn, Nucl. Phys. 37:554 (1962).
25. U. Mosel, Phys. Letters 46B:8 (1973).
26. E. Beth and G. Uhlenbeck, Physica 4:915 (1937).
27. R. Wolff, Diplomarbeit, Institut für Kernphysik, Technische Hochschule Darmstadt (1980).
28. T. Døssing, Cand. Scient. Thesis, Niels Bohr Institute, University of Copenhagen (1974); A. S. Jensen, private communication.
29. M. Beiner, Les Masses Nucléaires, Contributions aux IIIe Journées d'Etudes de la Division de Physique Théorique de l'I.P.N., Aussois (1971)
30. S. G. Nilsson and O. Prior, Mat. Fys. Medd. Dan. Vid. Selsk. 32, no. 16 (1961).
31. S. Bjørnholm, A. Bohr and B. R. Mottelson, Third Int. Conf. on the Physics and Chemistry of Fission, University of Rochester, paper IAEA/SM-174/205 (1973).
32. A. Bohr and B. R. Mottelson, Nuclear Structure Vol. 2 (Benjamin; New York) (1975).
33. F. Tondeur, Nucl. Phys. A315:353 (1979).
34. Y. Tanaka, Y. Oda, F. Petrovich and R. K. Sheline, Phys. Letters 83B:279 (1979).
35. B. C. Smith, F. N. Choudhury and S. Das Gupta, Phys. Rev. C17:318 (1978).
36. A. S. Jensen, private communication.
37. M. Beckerman, Nucl. Phys. A278:333 (1977).
38. M. Barranco and J. Treiner, Nucl. Phys. A351:269 (1980).
39. J. E. Lynn, The Theory of Neutron Resonance Reactions (Clarendon Press; Oxford) (1968).
40. H. Baba, Nucl. Phys. A159:625 (1970).
41. W. Dilg, W. Schantl, H. Vonach and M. Uhl, Nucl. Phys. A217:269 (1973).

DISCUSSION

J. Theobald: Mainly from excitation functions for photo fission one knows that the Bohr-Björnholm correction due to rotational level contributions gives rise to high level densities at high excitation energies ($E^* \gtrsim 10$ MeV). Therefore Ignatjeik had introduced an empirical function (q-function) to take out this correction with increasing excitation energy. If you subtract from the densities of your low temperature approach the ones of your high temperature approximation, do you find just this q function?

M. Armoult: This is an interesting point we did not look at up to now. However, it has to be stressed that only excitation energies $\lesssim 8$ MeV are involved in the comparison between theoretical estimates and the s-neutron resonance spacings (Fig. 1). In such conditions, the condition $t \ll \delta \hbar \omega_0$ is safely fulfilled, and the low temperature approximation (Eq. (19)) is not expected to drastically overestimate the level densities.

J. B. Wilhelmy: What is the magnitude of the collective enhancement effects in the rare earth and actinide region? Are these enhancements required to obtain adequate agreement with the experimental data?

M. Armoult: Typically, collective enhancements amount to factors of the order of 10-100. From Fig. 1 it can be seen that this enhancement is required in order to reach some agreement with the experimental data in the actinide region, as well as for the rare earths, except perhaps the heavier ones.